


RESEARCH

Open Access



Generating rectilinear motion using permanent magnets

Jihad Rishmany^{1*} , Guitta Sabiini², Ali Mansour¹ and Rodrigue Imad³

*Correspondence:
jihad.rishmany@balamand.edu.lb

¹ Department of Mechanical Engineering, University of Balamand, Al Koura, Lebanon

² Sabis International School, Adma, Lebanon

³ Department of Computer Engineering, University of Balamand, Al Koura, Lebanon

Abstract

This paper considers generating rectilinear motion using permanent magnets based on the surface charge method. In this regard, the existing analytical expressions of the interaction magnetic field between cuboidal permanent magnets are modified and extended into new ones that take into account the magnets configuration proposed in this work. The modified equations are then solved numerically and validated via experimental testing. Based on the obtained results, a case study is considered where a magnets configuration is set through numerical iterations to produce rectilinear motion. This configuration, validated experimentally, has a self-starting aspect and generates continuous motion. The proposed technique provides a simple and quick way to configure a set of magnets to produce rectilinear motion. Such systems could be used in various medical or industrial applications such as propelling nanobots throughout the soft tissue of the human body, or driving a production line. This offers a free source of energy resulting in power saving and reduced emissions.

Keywords: Surface charge method, Permanent magnets, Magnetic motion, Energy harvest

Introduction

Permanent magnets are now integrated in numerous aspects of everyday life and have many uses such as micro actuators, diamagnetic levitation devices, generation of remote fields for magnetic resonance imaging (MRI) or field gradients to sensors for mechanical data such as position or torque [14]. Moreover, converting the energy produced by permanent magnets (PMs) to electrical energy could be employed to operate small appliances and hence, hypothetically reduce the need for energy storage devices and power sources such as batteries and chargers. Furthermore, it is worth mentioning that with a large enough magnetic field, it would be possible to generate high amounts of electrical power which can help lessen carbon emissions [22, 26]. Accordingly, this would alleviate the problem of global warming. Various types of transducers have proven effective in converting the kinetic energy present in vibrations to electrical energy. Some of these transducers are; mechanical, magneto electric, electrostatic, electromagnetic, and piezoelectric [24]. Some of the methods that have been suggested in literature for harvesting energy directly from the human body rely on technologies like piezo electric generators, electrostatic vibration generators, thermo-generators, and electromagnetic rotational

generators amongst others [8]. Moreover, permanent magnets could benefit daily tasks in the industrial and medical fields by aiding in the displacement of objects. A good example in this context would be propelling nanobots throughout the soft tissue of the human body [22], or driving a production line forward.

Implementing the aforementioned applications requires a thorough understanding of the interaction between permanent magnets. This could be achieved by deriving the expressions of the magnetic field induced by such magnets.

There are two main types of permanent magnets which are commonly in use; parallelepipedic and cylindrical magnets. Parallelepipedic magnets are relatively simpler in terms of formulation of the magnetic field; consequently, they are treated in the present study.

Both numerical and analytical approaches [3, 5]) are employed to assess the behavior of permanent magnets. Numerical solutions are currently being used to accurately model complex geometries consisting of nonlinearities. Some of these methods include finite difference method (FDM) [6], finite element method (FEM) [11], and the boundary element method (BEM) [7]. However, the common problem with these methods is the extensive computational time [23]; hence analytical methods, which are relatively faster, are widely used.

Analytical approaches were proposed by Marinescu et al. [12] and analytical 2-D and 3-D solutions were given by Yonnet and Allag [25] and by Bancel and Lemarquand [4] for the magnetic field created by parallelepipedic magnets. Analytical magnetic field calculation techniques are either based on the harmonic method [8] coupled with Fourier series analysis [20], magnetic vector potential [21], 3D analytical method based on transfer relations [9], or the surface charge method [6, 24].

Van Dam et al. [24] suggested extending the surface charge method in order to enable multi-axial rotations to provide 6-DoF permanent magnet interaction model, which provides an analytical model which is faster than the already existing finite element method.

Due to the assumption of current free space, the charge model is only effective at modeling magnets. It can be used to effectively model cuboidal magnets in a short period of time [10] while also being able to model magnets having shapes other than the cuboidal, such as magnetic rings [15].

Neri [13] estimated the interaction force between permanent magnets and ferromagnetic target both for planar parallel surfaces and sloping surfaces. Ravaud et al. [16] presented a 3-D analytical calculation of the magnetic field due to permanent magnet rings using the Coulombian approach. Selvaggi et al. [18, 19] calculated the magnetic field produced by a set of permanent magnets in a permanent magnet motor. In order to model the geometry of the structure housing the magnets, a cylindrical coordinate system was used with the aid of Green's function to develop the expansion. In order to compute the equivalent point charge distribution, charge simulation method was used. Coulomb's law is applied in order to express the magnetic scalar potential in a mathematically tractable form.

The analytical surface charge method has been studied for decades now, dating back to 1984 when Akoun and Yonnet [2] first derived analytical equations which enabled the calculation of the magnetic field as well as the interaction force between two axially displaced PMs having parallel magnetization. The method was developed further as many

other researchers [27] worked on models which gave translational magnet arrangements for both cuboidal and cylindrical magnets [1, 15]). Some of these developments were equations which study the interaction between perpendicularly magnetized PMs for multi-axial displacements [10].

A different approach to calculating the force between cuboidal magnets is suggested by Zhang [26] where the force is calculated after assuming that the two cuboidal magnets to be two current loops and through this the resultant force between them would be calculated.

One of the principal problems that face circular magnets arrangement is surpassing the lock point created after the rotor completes a full rotation. Rashid et al. (Rashid, Yousaf and Ali 2013) [14] aimed at overcoming the lock point using an arrangement based on the two-media concept with different magnetic field permeability which reduces the opposition force produced at the lock point. This enables the rotor to overcome the lock point with the aid of its gained inertia. Once the lock point is passed, the magnetic field causes the rotor to accelerate once again.

In another attempt to surpass the lock-point and acquire a self-starting feature as well, Rishmany and Sabiini [17] designed a permanent magnet motor based on Baker's rotational magnetic propulsion device. However, since the continuity of the magnetic field was ensured by a continuously increasing stator, the output power of the system was very small compared to its size, which lead to a reduced efficiency.

In this work, an alternative configuration for a self-starting rectilinear motion of the rotor is proposed in order to obtain a continuously increasing magnetic field coupled with a significant output power and hence increased efficiency. This is achieved by employing an identical cuboidal magnet to form the stator and varying the relative distance between the stator magnets as well as the distance between the stator magnets and the rotor.

For that purpose, the analytical expressions of the magnetic field derived by Rishmany and Sabiini [17] are modified to take into account translational motion. Then, the system configuration is set through numerical iterations such that a continuously increasing magnetic field is obtained in the direction of motion. Finally, an experimental prototype is mounted and tested in order to validate the results.

Methods

The expressions of the magnetic field between two cuboidal magnets where the mobile magnet is idealized as a point $P(x,y,z)$ (Fig. 1) are given by [17]:

$$B_x = \begin{cases} \left[\frac{\mu_0 \cdot M}{4\pi} \ln \left(\frac{y + (y^2 + (x-a)^2 + z^2)^{1/2}}{(y-a) + ((y-a)^2 + (x-a)^2 + z^2)^{1/2}} \right) \right] \\ + \left[\frac{\mu_0 \cdot M}{4\pi} \ln \left(\frac{(y-a) + ((y-a)^2 + x^2 + z^2)^{1/2}}{y + (y^2 + x^2 + z^2)^{1/2}} \right) \right] \\ + \left[\frac{\mu_0 \cdot M}{4\pi} \ln \left(\frac{(y-a) + ((y-a)^2 + (x-a)^2 + (z+a)^2)^{1/2}}{y + (y^2 + (x-a)^2 + (z+a)^2)^{1/2}} \right) \right] \\ + \left[\frac{\mu_0 \cdot M}{4\pi} \ln \left(\frac{y + (y^2 + x^2 + (z+a)^2)^{1/2}}{(y-a) + ((y-a)^2 + x^2 + (z+a)^2)^{1/2}} \right) \right] \end{cases} \quad (1)$$

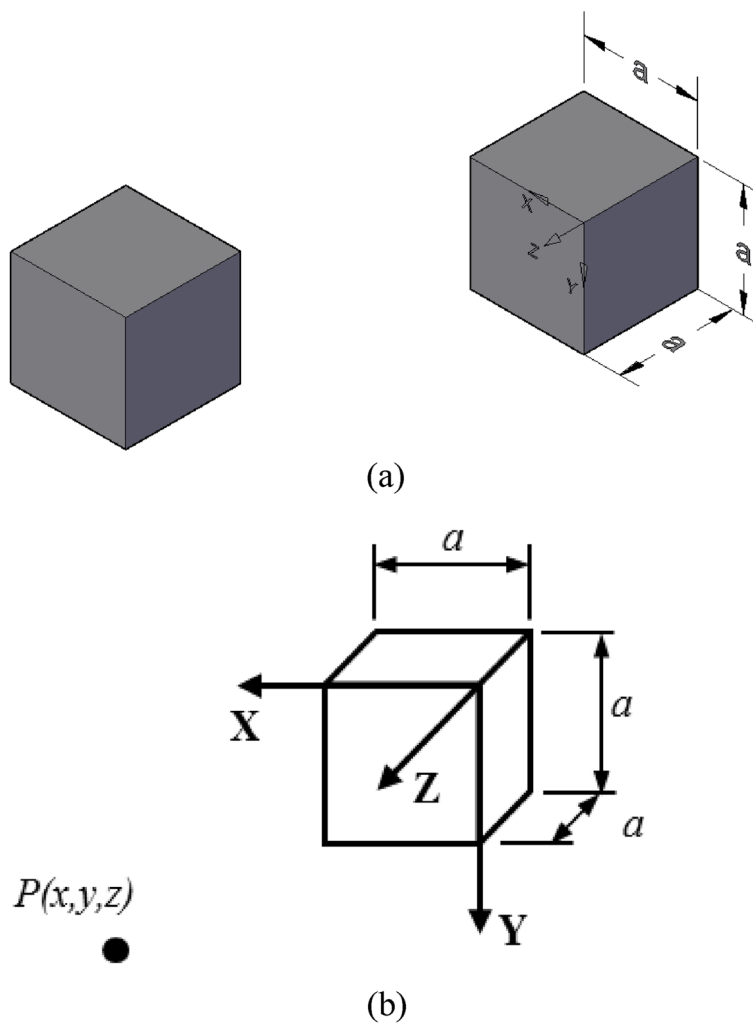


Fig. 1 Schematic drawing of cuboidal magnets, **a** real model, **b** idealized model

$$B_z = \frac{\mu_0 M}{4\pi} \left\{ \begin{aligned} & - \tan^{-1} \left(\frac{(y-a)(x-a)}{(z+a)\sqrt{(x-a)^2 + (y-a)^2 + (z+a)^2}} \right) \\ & + \tan^{-1} \left(\frac{(y-a)x}{(z+a)\sqrt{x^2 + (y-a)^2 + (z+a)^2}} \right) \\ & + \tan^{-1} \left(\frac{y(x-a)}{(z+a)\sqrt{(x-a)^2 + y^2 + (z+a)^2}} \right) \\ & + \tan^{-1} \left(\frac{yx}{(z+a)\sqrt{x^2 + y^2 + (z+a)^2}} \right) \end{aligned} \right. \quad (2)$$

Since only plane motion is considered, the expression of B_y is irrelevant.

Generalizing Eqs. (1) and (2) to take into account an arbitrary positioning of the stators (Fig. 2):

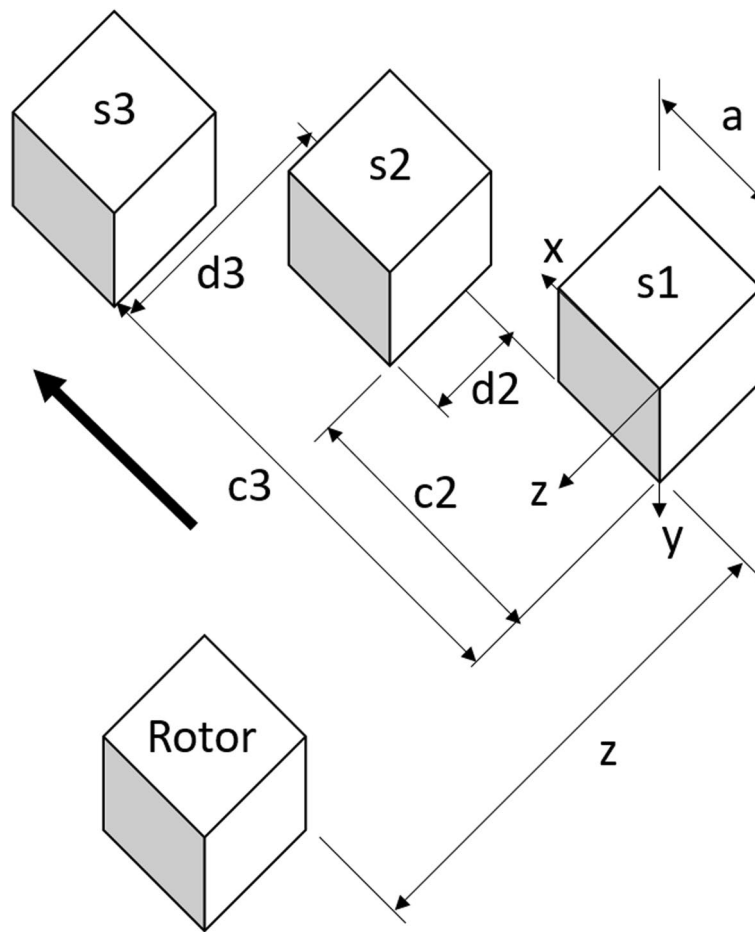


Fig. 2 Magnet configuration comprising a rotor and a set of identical stators

$$B_x = \frac{\mu_0 \cdot M}{4\pi} \left\{ \begin{aligned} & \ln \left(\frac{y + (y^2 + (x - c_i - a)^2 + (z - d_i)^2)^{1/2}}{(y - a) + ((y - a)^2 + (x - c_i - a)^2 + (z - d_i)^2)^{1/2}} \right) \\ & + \ln \left(\frac{(y - a) + ((y - a)^2 + (x - c_i)^2 + (z - d_i)^2)^{1/2}}{y + (y^2 + (x - c_i)^2 + (z - d_i)^2)^{1/2}} \right) \\ & + \ln \left(\frac{(y - a) + ((y - a)^2 + (x - c_i - a)^2 + (z + a - d_i)^2)^{1/2}}{y + (y^2 + (x - c_i - a)^2 + (z + a - d_i)^2)^{1/2}} \right) \\ & + \ln \left(\frac{y + (y^2 + (x - c_i)^2 + (z + a - d_i)^2)^{1/2}}{(y - a) + ((y - a)^2 + (x - c_i)^2 + (z + a - d_i)^2)^{1/2}} \right) \end{aligned} \right. \quad (3)$$

$$B_z = \frac{\mu_0 M}{4\pi} \left\{ \begin{array}{l} \tan^{-1} \left(\frac{(y-a)(x-a-c_i)}{(z-d_i)\sqrt{(x-a-c_i)^2 + (y-a)^2 + (z-d_i)^2}} \right) \\ - \tan^{-1} \left(\frac{(y-a)(x-c_i)}{(z-d_i)\sqrt{(x-c_i)^2 + (y-a)^2 + (z-d_i)^2}} \right) \\ - \tan^{-1} \left(\frac{y(x-a-c_i)}{(z-d_i)\sqrt{(x-a-c_i)^2 + y^2 + (z-d_i)^2}} \right) \\ + \tan^{-1} \left(\frac{y(x-c_i)}{(z-d_i)\sqrt{(x-c_i)^2 + y^2 + (z-d_i)^2}} \right) \\ - \tan^{-1} \left(\frac{(y-a)(x-a-c_i)}{(z+a-d_i)\sqrt{(x-a-c_i)^2 + (y-a)^2 + (z+a-d_i)^2}} \right) \\ + \tan^{-1} \left(\frac{(y-a)(x-c_i)}{(z+a-d_i)\sqrt{(x-c_i)^2 + (y-a)^2 + (z+a-d_i)^2}} \right) \\ + \tan^{-1} \left(\frac{y(x-a-c_i)}{(z+a-d_i)\sqrt{(x-a-c_i)^2 + y^2 + (z+a-d_i)^2}} \right) \\ - \tan^{-1} \left(\frac{y(x-c_i)}{(z+a-d_i)\sqrt{(x-c_i)^2 + y^2 + (z+a-d_i)^2}} \right) \end{array} \right. \quad (4)$$

where c_i and d_i define the position of magnet i of the stator with respect to the origin of axes.

Experimental validation

In order to validate the derived expressions, two sets of measurements were conducted. The first consisted of placing a magnet on a 2 mm graduated paper and measuring via a teslameter the intensity of the magnetic field at various locations (Fig. 3).

The second experiment consisted of placing two magnets between the grips of the Universal Test Machine (UTM) (Fig. 4) and a tensile test was conducted. The magnets are positioned such that the free faces are opposite in magnetization and hence would induce an attractive force between them. The relative position of the magnets is measured, and the test is run at a constant velocity of 10 mm/s. The stress–strain diagram obtained from the UTM software is then adjusted to produce the force as a function of the distance between the magnets. Finally, the interaction magnetic field between the magnets is deduced and the obtained results are compared with the analytical curve (Fig. 5).

The Mean Square Error (MSE) between experimental and analytical results is computed as follows and plotted on Fig. 6:

$$MSE = (B_{z,\text{analytical}} - B_{z,\text{experimental}})^2$$

Figure 6 shows a good agreement between analytical and experimental results.

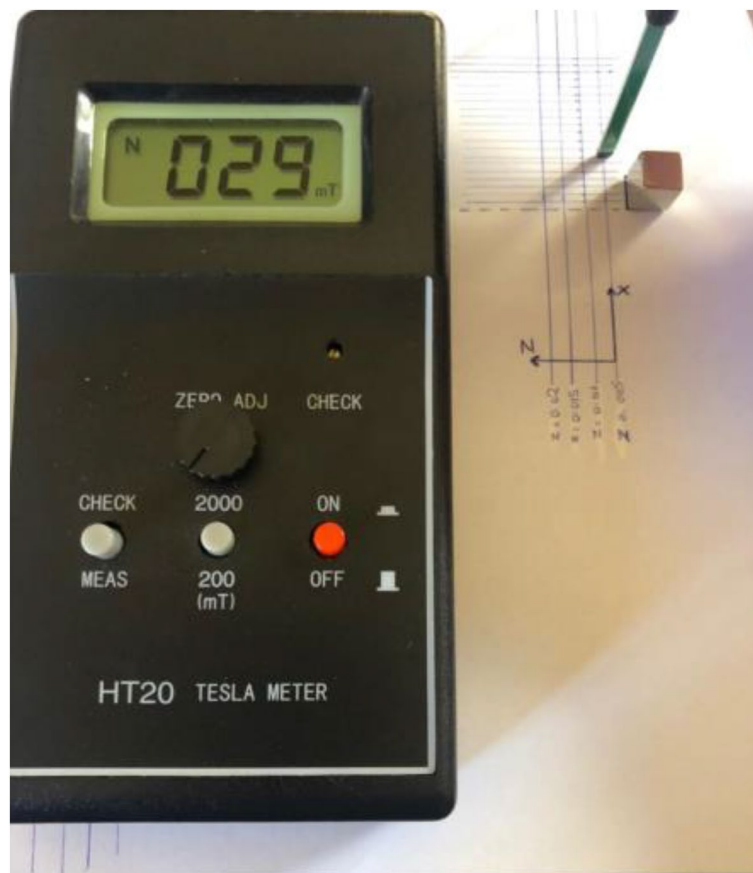


Fig. 3 Measurement of the magnetic field between a point and a magnet at various locations

Results and discussion

Based on the expressions of the magnetic field derived previously, numerical iterations are conducted in order to configure a magnets arrangement capable of producing a continuous rectilinear motion starting from rest (Fig. 7).

For that purpose, consider a set of permanent cuboidal Ne52 magnets of side a . The magnets forming the stator are all positioned symmetrically with respect to a linear track where the movable magnet (labelled Rotor) is placed.

Fixing the configuration requires finding the distances c_1, c_2, \dots, c_7 and d_1, d_2, \dots, d_7 in order to achieve a continuous rotor movement from bottom to top.

In order to locate the position of the first magnet with respect to the rotor, the 2 magnets are placed facing each other and the interaction magnetic field components B_x and B_z are plotted in function of z (Fig. 8).

B_z decreases rapidly as the distance between the two magnets increases, reaching zero at about 3 cm. On the other hand, B_x is less affected and decreases by almost 30% of its initial value within a distance of 5 cm.



Fig. 4 Experimental measurement of the magnetic force using the UTM

The distance between the remaining stators and the track should decrease progressively in order to obtain an increasing resultant magnetic field ($B_{x,res}$) in the presumed direction of motion. This is achieved through a numerical iterations based on trial and error where the positions of stators are varied until the required variation of $B_{x,res}$ is obtained (Fig. 9).

The continuous positive slope of $B_{x,res}$ implies that the rotor will experience continuous rectilinear motion in the X-direction along the rotor track.

Once configured, the arrangement is tested experimentally by creating a rotor track and fixing the stators in their corresponding position on both sides of the track (Fig. 10).

The corresponding parameters related to the proposed configuration are listed in Table 1.

In this configuration, identical cubic magnets were placed at varying distances in the X and Z directions in order to create a resultant magnetic field which gradually increases

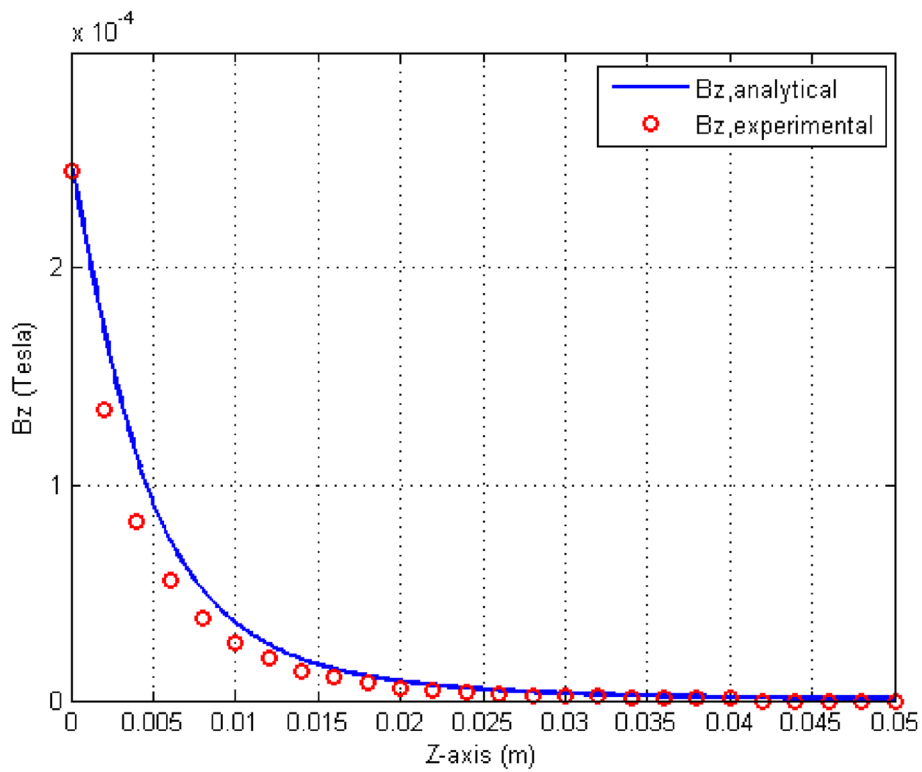


Fig. 5 Comparison between experimental and analytical results of the interaction magnetic field between two magnets

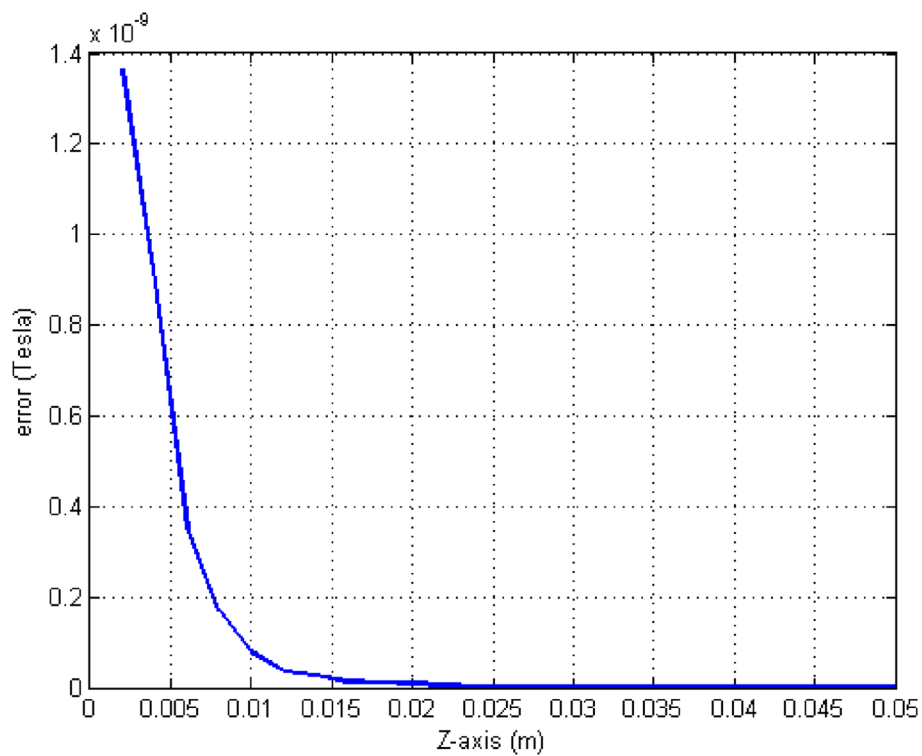


Fig. 6 Mean square error between experimental and analytical results for the interaction magnetic field between two magnets

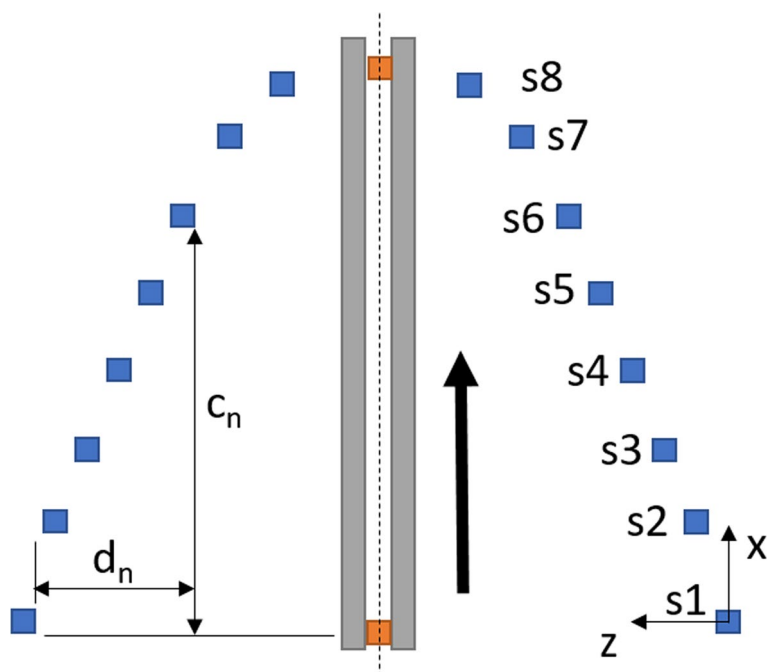


Fig. 7 Schematic drawing of the magnets configuration for continuous rectilinear motion

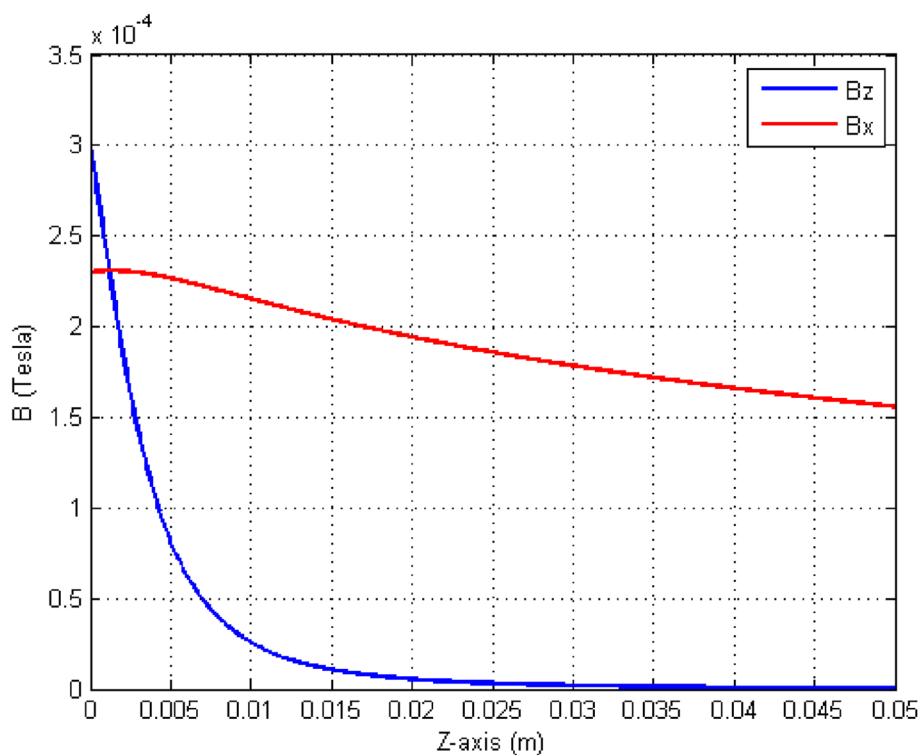


Fig. 8 Variation of B_z and B_x as a function of Z

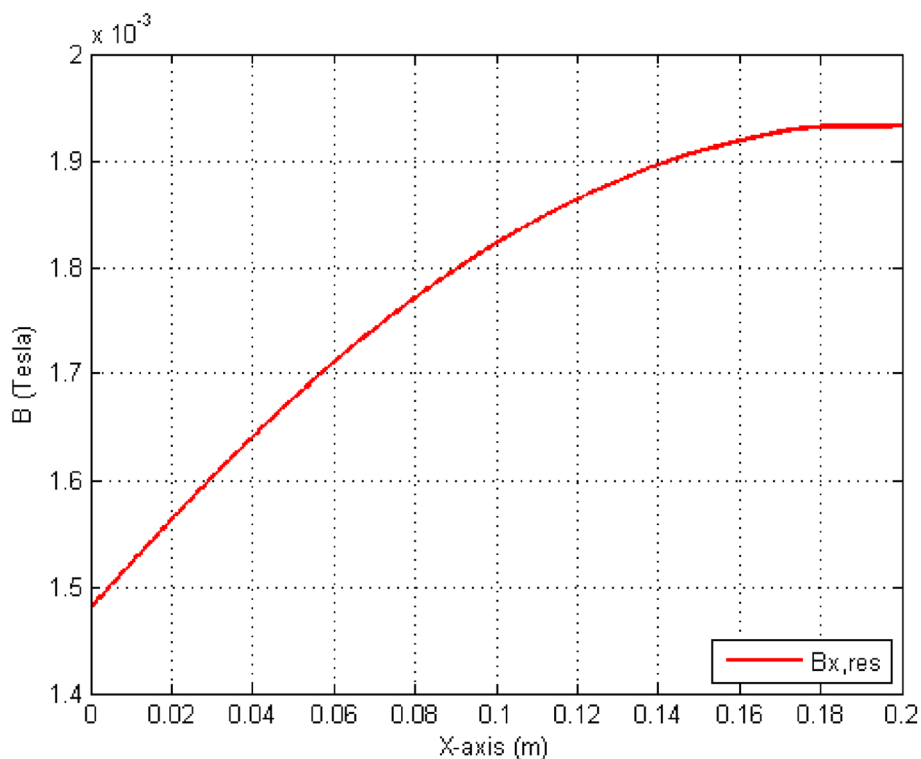


Fig. 9 Resultant magnetic field ($B_{x,res}$) between the rotor and the stator magnets

from the first set of stators till the last. This was done in order to achieve a continuous rectilinear motion of the rotor. The first set of stators are placed furthest away from the rotor track and the distance for the remaining sets of stators is gradually decreased.

Conclusions

The main aim of this study is to develop an analytical formulation of the interaction magnetic field between two cuboidal magnets. Gaining a better understanding of how this interaction occurs will help open up a new promising field when it comes to designing and optimizing devices which depend on magnetic forces interaction for operation. This provides a source of eco-friendly energy which can be used in a wide range of applications in order to help alleviate the worldwide crisis of global warming and reduce harmful emissions.

The analytical expressions are obtained using the surface charge method, and verified experimentally through two different approaches. The first consisted of measuring, using a teslameter, the intensity of the magnetic field at different locations from a fixed magnet. The second approach relied on the UTM machine in order to plot the interaction magnetic force between two magnets as a function of the axial distance between them.

The derived equations are further embedded in a MATLAB code. Then, a trial and error approach is employed in order to design a magnets configuration capable of

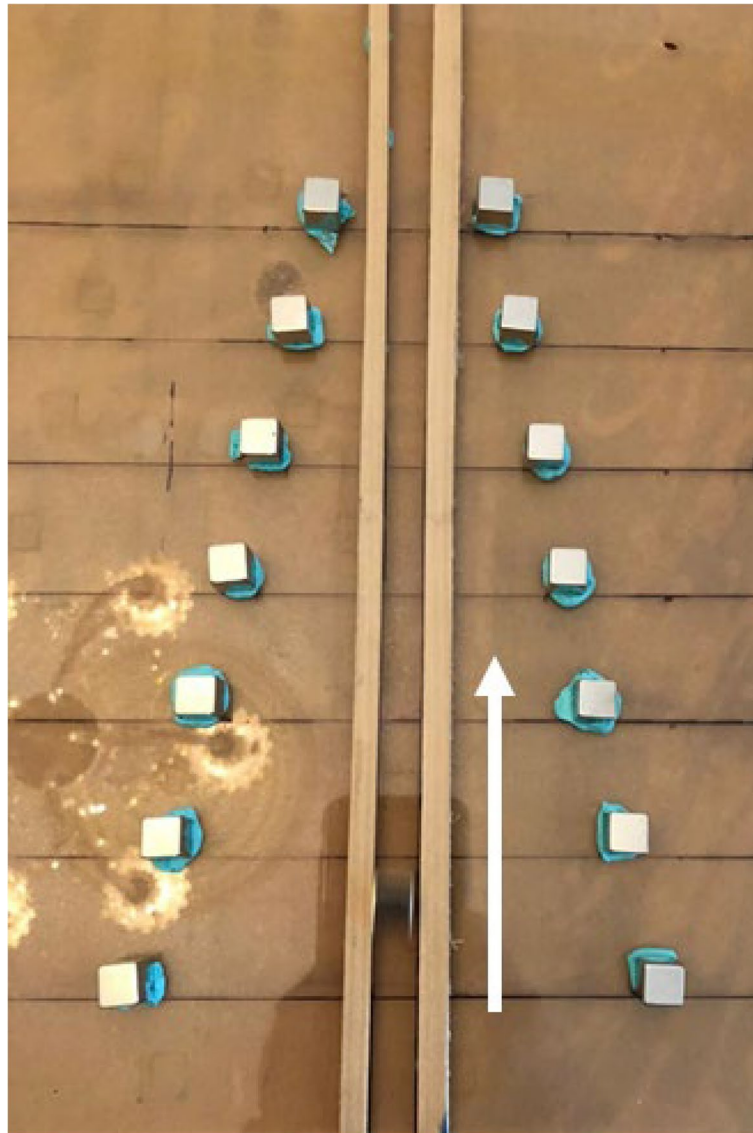


Fig. 10 Experimental setup for continuous rectilinear motion

generating a continuous rectilinear motion along a set track. This design is comprised of a set of identical permanent magnets placed symmetrically at either side of the track. The distance between the magnets and the track decreases gradually in the presumed direction of motion. This creates an increasing magnetic field, and hence resultant force, in the direction of motion, which leads to a continuous rectilinear motion of the rotor along the track. The modeled configuration was then tested experimentally; the result was the rotor experiencing continuous rectilinear motion starting from test.

The method developed in this work provides a simple and quick way to configure a set of magnets to produce rectilinear motion. Such systems could be easily scaled and hence

Table 1 Parameters used for the proposed configuration

Parameter	Value
Magnetization (M)	1000 A/m
μ_0	$4\pi \times 10^{-7} \text{Tm/A}$
Magnet side (a)	1 cm
c1	0
c2	3.33 cm
c3	6.66 cm
c4	10 cm
c5	13.32 cm
c6	16.65 cm
c7	20 cm
d1	0
d2	0.66 cm
d3	1.32 cm
d4	2 cm
d5	2.64 cm
d6	3.33 cm
d7	4 cm

be used in small-scale applications such as propelling nanobots throughout the soft tissue of the human body, or in large-scale applications such as driving a production line.

Potential improvements include finding the required expressions that enable configuring a system providing continuous rotational motion. Such systems would generate clean energy which could be used to operate small appliances.

Abbreviations

PM Permanent magnet
UTM Universal testing machine

Acknowledgements

N/A.

Authors' contributions

JR proposed the topic, established the mathematical modeling, conducted the numerical simulations, set the experimental setup, and post-processed the results. GS derived and solved the mathematical equations. AM conducted the experimental testing and the CAD drawings. RI did the state of the art study. JR and AM contributed to the writing of the manuscript. All authors have read and approved the manuscript.

Funding

The authors did not receive support from any organization for the submitted work.

Availability of data and materials

The datasets generated during and/or analysed during the current study are available from the corresponding author on reasonable request.

Declarations

Competing interests

The authors declare that they have no conflict of interest.

Received: 20 January 2023 Accepted: 30 May 2023

Published online: 05 June 2023

References

1. Agashe JS, Arnold DP (2008) A study of scaling and geometry effects on the forces between cuboidal and cylindrical magnets using analytical force solutions. *J Phys D Appl Phys* 41(10):105001
2. Akoun G, Yonnet J-P (1984) 3D analytical calculation of the forces exerted between two cuboidal magnets. *IEEE Trans Magn* 20(5):1962–1964
3. Allag H, Yonnet JP, Fassenet M, Latreche ME (2009) 3D analytical calculation of interactions between perpendicularly magnetized magnets—application to any magnetization direction. *Sens Lett* 7(3):486–491
4. Bancel F, Lemarquand G (1998) Three-dimensional analytical optimization of permanent magnets alternated structure. *IEEE Trans Magn* 34(1):242–247
5. Charpentier JF, Lemarquand G (1999) Study of permanent-magnet couplings with progressive magnetization using an analytical formulation. *IEEE Trans Magn* 35(5):4206–4217
6. Furlani EP (2001) Permanent magnet and electromechanical devices: materials, analysis, and applications. United States: Academic Press. eBook ISBN: 9780080513690
7. Gaul L, Kögl M, Wagner M (2004) Boundary element methods for engineers and scientists: an introductory course with advanced topics. *Appl Mech Rev* 57(6):B31–B31
8. Hague B (1929) Electromagnetic Problems in Electrical Engineering: An Elementary Treatise on the Application of the Principles of Electromagnetism to the Theory of the Magnetic Field and of the Mechanical Forces in Electrical Machinery and Apparatus. *H. Milford*
9. Jang GH, Koo MM, Kim JM, Choi JY (2017) Torque characteristic analysis and measurement of axial flux-type non-contact permanent magnet device with Halbach array based on 3D analytical method. *AIP Adv* 7(5):056647
10. Janssen JLG, Paulides JH, Lomonova EA (2011) 3-D analytical calculation of the torque between perpendicular magnetized magnets in magnetic suspensions. *IEEE Trans Magn* 47(10):4286–4289
11. Jin J (2002) The finite element method in electromagnetics. New York: Wiley. 1993 p. 753
12. Marinescu M, Marinescu N (1989) Compensation of anisotropy effects in flux-confining permanent-magnet structures. *IEEE Trans Magn* 25(5):3899–3901
13. Neri P (2019) Interaction force between magnetic field and ferromagnetic target: analytical, numerical and experimental study. *Simulation* 95(3):209–218
14. Rashid A, Yousaf K, Ali Z (2013) Theory of permanent magnetic motion and variable field permanent magnetic motor. *Arab J Sci Eng* 38(10):2755–2764. <https://doi.org/10.1007/s13369-012-0485-x>
15. Ravaut R, Lemarquand G, Lemarquand V (2009) Force and stiffness of passive magnetic bearings using permanent magnets. Part 1: axial magnetization. *IEEE Trans Magn* 45(7):2996–3002
16. Ravaut R, Lemarquand G, Lemarquand V (2009) Magnetic field created by tile permanent magnets. *IEEE Trans Magn* 45(7):2920–2926
17. Rishmany J, Sabiini G (2019) Interaction magnetic field formulation of permanent magnets based on Baker's rotational magnetic propulsion device. *Int J Electr Hybrid Veh* 11(2):152–169
18. Selvaggi JP, Salon S, Kwon OM, Chari MVK (2004) Calculating the external magnetic field from permanent magnets in permanent-magnet motors-an alternative method. *IEEE Trans Magn* 40(5):3278–3285
19. Selvaggi JP, Salon SJ, Chari MV (2010) Employing toroidal harmonics for computing the magnetic field from axially magnetized multipole cylinders. *IEEE Trans Magn* 46(10):3715–3723
20. Shin KH, Cho HW, Choi JY (2017) Experimental verification and analytical calculation of unbalanced magnetic force in permanent magnet machines. *AIP Adv* 7(5):056652
21. Shin KH, Park HI, Cho HW, Choi JY (2017) Parametric analysis and optimized torque characteristics of a coaxial magnetic gear based on the subdomain analytical model. *AIP Adv* 7(5):056619
22. Son D, Ugurlu MC, Sitti M (2021) Permanent magnet array-driven navigation of wireless millirobots inside soft tissues. *Sci Adv* 7(43):eabi8932
23. Van Casteren DTEH, Paulides JH, Lomonova EA (2014) 3-D numerical surface charge model including relative permeability: the general theory. *IEEE Trans Magn* 50(11):1–4
24. Van Dam JRM, Paulides JH, Lomonova EA, & Dhaens M (2015) Machine and actuator design: modeling 3-D fields and forces using the analytical surface charge expressions. In: 2015 International Conference on Sustainable Mobility Applications, Renewables and Technology (SMART). IEEE p 1-5
25. Yonnet JP, Allag H (2011) Three-dimensional analytical calculation of permanent magnet interactions by “magnetic node” representation. *IEEE Trans Magn* 47(8):2050–2055
26. Zhang Y, Leng Y, Zhang H, Su X, Sun S, Chen X, Xu J (2020) Comparative study on equivalent models calculating magnetic force between permanent magnets. *J Intell Manuf Special Equip* 1(1):43–65. <https://doi.org/10.1108/JIMSE-09-2020-0009>
27. Zhang H, Kou B, Zhou L (2020) An improved surface charge model for the static force calculation among the permanent magnets in magnetic bearings or magnetic springs. *IEEE Trans Magn* 57(2):1–4

Publisher's Note

Springer Nature remains neutral with regard to jurisdictional claims in published maps and institutional affiliations.